Analysis of Multilayer Microstrip Lines by a Conformal Mapping Method

Jiří Svačina

Abstract—**The article contains an investigation of multilayer microstrip transmission lines. The conformal mapping method is used to obtain simple analytical relations for the filling factors and the effective permittivity of two fundamental types of three-layer microstrips. Numerical results obtained by the present method are compared with available data from other authors.**

I. Introduction

The multilayer microstrip line is a stripline whose cross section is filled with several layers of different dielectrics of different permittivity ϵ_r. In the following the individual dielectric layers will be assumed to be linear, homogenous and isotropic.

The properties of multilayer microstrip lines can be investigated by various methods. In [2] and [3] the authors used a method based on variational calculus, while the authors of [4] start from the numerical determination of Green's function for a given problem. Both methods provide sufficiently accurate results, although they require a comparatively long computation time. A common disadvantage of these methods—as with all numerical methods—is that they do not provide a clear analytic review of the effect of geometrical dimensions and technological line constants on the electrical parameters of microstrip. This disadvantage is removed by an approximate analytical method using the conformal mapping method.

The principles of using the conformal mapping method for the solution of microstrip lines have been described in detail in many publications, e.g., [1], [5], [6]. Assuming the quasi-TEM wave propagation in the line investigated, it is obvious that the existence of more layers of different dielectrics will only alter the effective permittivity of a multilayer microstrip while the dimensional relations obtained by the conformal transformation will not be changed by the presence of a multilayer dielectric. When solving various types of multilayer lines, we will, in principle, follow the conformal transformations used already by Wheeler in his classical works [5] and [6].

II. Three-Layer Microstrip Line of the First Type

This type of three-layer structure (Fig. 1(a)) will be conformally mapped with the help of the Wheeler's transformation [5] from the complex variable plane $z = x + j \cdot y$ onto another plane $g = u + j \cdot v$ with the results as shown in Fig. 1(b). We will also transform the individual interfaces between dielectric layers ϵ_{r1} and ϵ_{r2}, or ϵ_{r2} and ϵ_0. The degree of filling the cross section of a microstrip line in a g-plane by individual dielectrics ϵ_{r1} and ϵ_{r2} is characterized by a filling factor q_1, or q_2, which, according to [6], is defined by the ratio of the area $S_{\epsilon 1}$ ($S_{\epsilon 2}$) taken up in the cross section by the respective dielectric and the whole area S_C of the cross section in the

Manuscript received June 26, 1991; revised October 18, 1991.

The author is with the Department of Radioelectronics, Faculty of Electrical Engineering, Technical University of Brno, Antoninska 1, 662 09, Brno, Czechoslovakia.

IEEE Log Number 9106041.

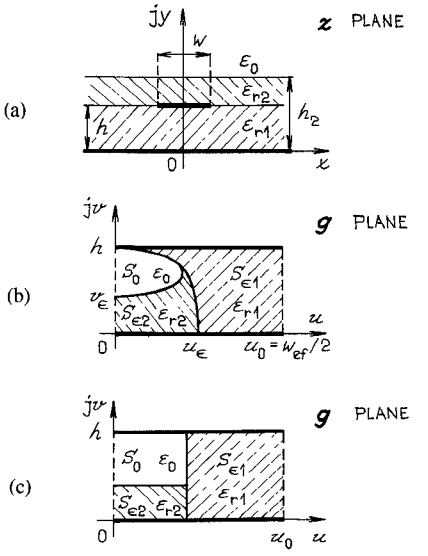

Fig. 1. Three-layer microstrip line of the first type.

g-plane. Then we have

$$q_1 = \frac{S_{\epsilon 1}}{S_C} = \frac{S_C - S_0 - S_{\epsilon 2}}{S_C} = 1 - \frac{S_0 + S_{\epsilon 2}}{S_C}, \tag{1}$$

$$q_2 = \frac{S_{\epsilon 2}}{S_C} = \frac{S_C - S_{\epsilon 1} - S_0}{S_C} = 1 - \frac{S_{\epsilon 1}}{S_C} - \frac{S_0}{S_C} = 1 - q_1 - \frac{S_0}{S_C}. \tag{2}$$

The boundary curves of areas S_0 and $S_{\epsilon 2}$ (Fig. 1(b)) can be approximated with a high degree of accuracy by elliptical segments. Thus when using Wheeler's transformation for a wide microstrip line ($w/h \geq 1$), we can derive for the filling factors:

$$q_1 = 1 - \frac{1}{2} \cdot \frac{\ln\left(\frac{\pi}{h} w_{ef} - 1\right)}{\frac{w_{ef}}{h}}, \tag{3}$$

$$q_2 = 1 - q_1 - \frac{1}{2} \cdot \frac{h - v_\epsilon}{w_{ef}} \cdot \ln\left[\pi \frac{w_{ef}}{h} \frac{\cos\left(\frac{v_\epsilon}{2} \cdot \frac{\pi}{h}\right)}{\pi\left(\frac{h_2}{h} - \frac{1}{2}\right) + \frac{v_\epsilon}{2} \cdot \frac{\pi}{h}} + \sin\left(\frac{v_\epsilon}{2} \cdot \frac{\pi}{h}\right)\right], \tag{4}$$

where the effective line width is

$$w_{ef} = w + \frac{2h}{\pi} \ln\left[17.08\left(\frac{w}{2h} + 0.92\right)\right] \tag{5}$$

and the quantity v_ϵ is given as

$$v_\epsilon = 2\frac{h}{\pi} \operatorname{arctg}\left[\frac{\pi}{\frac{\pi}{2}\frac{w_{ef}}{h} - 2}\left(\frac{h_2}{h} - 1\right)\right]. \tag{6}$$

In the case of narrow microstrip lines ($w/h \leq 1$) it is necessary to use other mathematical functions for conformal mapping [1].

Then the filling factors are

$$q_1 = \frac{1}{2} + \frac{0.9}{\pi \cdot \ln \frac{h}{w}}, \tag{7}$$

$$q_2 = \frac{1}{2} - \frac{0.9 + \frac{\pi}{4} \ln\left(\frac{h_2/h + 1}{h_2/h + w/4h - 1}\right) \cdot \arccos\left\{\left[1 - \frac{h}{h_2}\left(1 - \frac{w}{8h}\right)\right]\sqrt{\frac{h_2/h + 1}{h_2/h + w/4h - 1}}\right\}}{\pi \cdot \ln \frac{8h}{w}}. \tag{8}$$

To determine the effective permittivity of the three-layer microstrip in Fig. 1(a) we substitute as a first approximation the individual dielectric areas in Fig. 1(b) by the structure in Fig. 1(c). The character of the boundary curves of the individual areas really allows such a substitution, while the areas $S_{\epsilon 1}$, $S_{\epsilon 2}$, and S_0 remain unchanged. From the arrangement in Fig. 1(c) we derive a relation for effective permittivity:

$$\epsilon_{efr} = \epsilon_{r1} q_1 + \epsilon_{r2} \cdot \frac{(1 - q_1)^2}{\epsilon_{r2}(1 - q_1 - q_2) + q_2}. \tag{9}$$

The corresponding value of characteristic impedance is calculated as

$$Z_0 = \frac{120\pi}{\sqrt{\epsilon_{efr}}} \cdot \frac{h}{w_{ef}} \tag{10}$$

for a wide line, $w/h \geq 1$, and

$$Z_0 = \frac{60}{\sqrt{\epsilon_{efr}}} \cdot \ln \frac{8h}{w}. \tag{11}$$

for a narrow line, $w/h \leq 1$.

The accuracy of the relations derived was compared with values of Z_0 taken from [4] for $\epsilon_{r1} = 9.6$ and $\epsilon_{r2} = 2.6$. In the whole range of the ratio $0.25 \leq w/h \leq 3.5$ the results of both calculations in Fig. 2 differ by less than 2% and in a substantial part of the range by less than 1%. However the real divergence can be even less by taking into consideration possible inaccuracies in reading the graph in [4].

In [8], the investigation of an inverted microstrip is made. Any comparison our results with those in [8] are given in Fig. 3. It indicate that the agreement between both methods of computations is reasonably good and the errors between measured and our computed values of $\sqrt{\epsilon_{efr}}$ are within 2 percent over the given range of aspect ratios w/h. Fig. 3 also shows computed values of $\sqrt{\epsilon_{efr}}$ based on a closed form equations for inverted microstrip given in [9]. Its accuracy is obviously less than this of the present method. Moreover, our expressions are more simple and easy to survey.

III. Three-Layer Microstrip Line of Second Type

In this type of microstrip (Fig. 4(a)) the area between the strips is composed of two different dielectrics ϵ_{r1} and ϵ_{r2} while above the upper strip there is air of permittivity ϵ_0. With the aid of a conformal transformation of the interface between the dielectrics into a complex g-plane, we can derive relations for the filling factors q_1 and q_2. For wide microstrip ($w/h \geq 1$), we obtain

$$q_1 = \frac{S_{\epsilon 1}}{S_C} = \frac{1}{2} \cdot \frac{h_1}{h}\left[1 + \frac{\pi}{4} - \frac{h}{w_{ef}} \ln\left(\frac{\pi}{h} \cdot w_{ef} \frac{\sin\left(\frac{\pi}{2}\frac{h_1}{h}\right)}{\frac{\pi}{2} \cdot \frac{h_1}{h}} + \cos\left(\frac{\pi}{2}\frac{h_1}{h}\right)\right)\right], \tag{12}$$

$$q_2 = \frac{S_{\epsilon 2}}{S_C} = 1 - q_1 - \frac{1}{2} \cdot \frac{\ln\left(\frac{\pi}{h} w_{ef} - 1\right)}{\frac{w_{ef}}{h}}, \tag{13}$$

in which the effective width of microstrip w_{ef} is given by (5). For narrow microstrip ($w/h \leq 1$), we have

$$q_1 = \frac{\ln \frac{1 + \frac{h_1}{h}}{1 - \frac{h_1}{h} + \frac{w}{4h}}}{2 \cdot \ln \frac{8h}{w}} \cdot \left[1 + \frac{\pi}{4} - \frac{1}{2}\arccos\left(\frac{h}{h_1} \cdot \frac{w}{8h}\sqrt{\frac{1 + \frac{h_1}{h}}{1 - \frac{h_1}{h} + \frac{w}{4h}}}\right)\right], \tag{14}$$

$$q_2 = \frac{1}{2} + \frac{0.9}{\pi \cdot \ln \frac{8h}{w}} - q_1. \tag{15}$$

Owing to the predominant character of the lines dividing the individual dielectric areas in Fig. 4(b), it is possible to substitute the cross section of lines in the g-plane by an approximately equivalent structure in Fig. 4(c). From this the effective permittivity is given as

$$\epsilon_{efr} = 1 - q_1 - q_2 + \epsilon_{r1}\epsilon_{r2} \cdot \frac{(q_1 + q_2)^2}{\epsilon_{r1} q_2 + \epsilon_{r2} q_1}. \tag{16}$$

The solid line in Fig. 5 gives the calculated result of the characteristic impedance of the three-layer microstrip of the second type with parameters $\epsilon_{r1} = 12$, $\epsilon_{r2} = 4.5$ and $h/h_1 = 1.01$ (the thickness of the upper strip $t = 0$). For comparison the curve taken from [2] is drawn as a dashed line. It is obvious that in the range $w/h \geq 1$ the agreement of both curves is very good (the divergence is less than 1%), for $w/h \leq 1$ their divergence increases up to value of about 3.5% when $w/h = 0.1$.

In Fig. 6(a) is shown a suspended microstrip line with parameters $\epsilon_{r1} = 1$, $\epsilon_{r2} = 2.55$, $w = 5.2$ mm and $t = 0.2$ mm. Such a

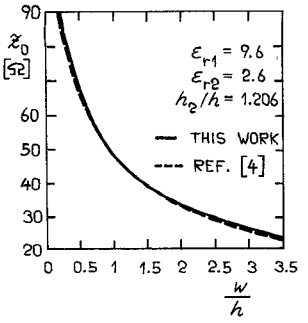

Fig. 2. Characteristic impedance of three-layer microstrip, first type.

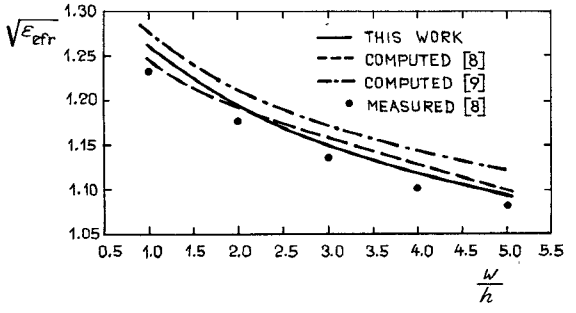

Fig. 3. Parameters of inverted microstrip (h = 0.381 mm, h_2 = 0.889 mm, $\epsilon_{r1} = 1$, $\epsilon_{r2} = 3.78$, t = 6.35 μm).

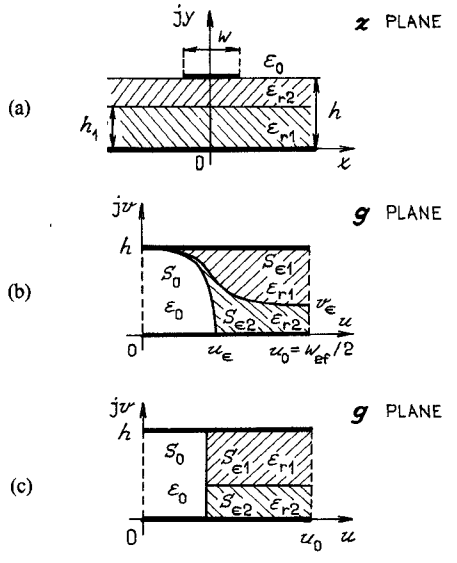

Fig. 4. Three-layer microstrip line of the second type.

structure with the height $h = h_1 + 4.9$ mm, was investigated in [2]. The distance h_1 being changed in integer multiples of the basic value h_{10} = 3.05 mm. In Fig. 6(b) the dependence of the capacitance per unit of this line on the ratio h_1/h_{10} is described. Besides our result (solid line), Fig. 6(b) also gives the curve calculated by the author of [2] (dashed line) and his experimentally established values (discrete points) at a frequency of 1.5 MHz.

A similar comparison is also given in Fig. 6(c) for the value $\lambda_g/\lambda_0 = 1/\sqrt{\epsilon_{efr}}$. Since the experimental values were found at a frequency of 4 GHz, it was necessary, when using relations (16), to introduce a frequency correction of the effective permittivity. To do this we used the expression for frequency dependence ϵ_{efr} ac-

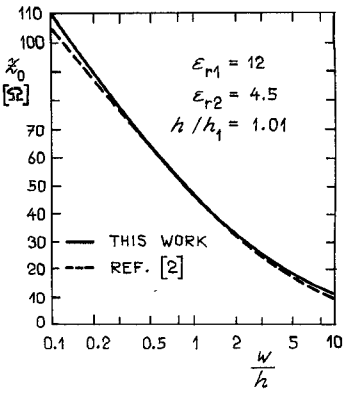

Fig. 5. Characteristic impedance of three-layer microstrip, second type.

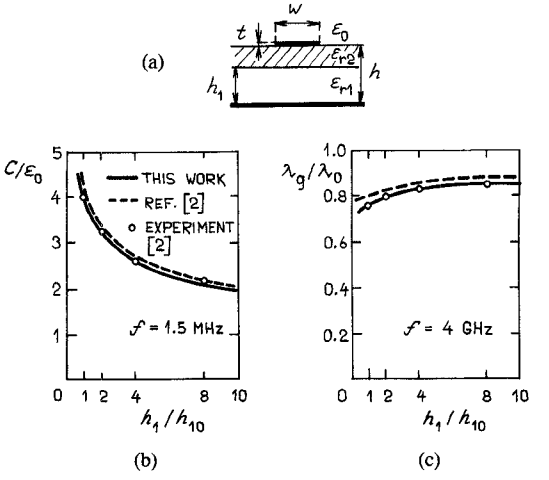

Fig. 6. Parameters of microstrip line with suspended substrate ($\epsilon_{r1} = 1$, $\epsilon_{r2} = 2.55$, w = 5.2 mm, t = 0.2 mm, $h - h_1$ = 4.9 mm, h_{10} = 3.05 mm).

cording to Getsinger [7]. It is obvious from Fig. 6(c) and Fig. 6(b) that the values calculated by the present method are practically identical with the measured values. Moreover, the experimental values given are obviously very accurate because both the capacitance C per unit of the line at low frequencies (1.5 MHz), and the wavelength λ_g of the line can be measured with considerable accuracy.

Closed form expressions for a suspended microstrip are available in [9], but the results obtained from this are incorrect (for instance: the effective permittivity of a suspended microstrip calculated from these expressions decreases with increasing of the aspect ratio w/h).

IV. Conclusion

The analysis given in this article has shown that the conformal mapping method provides good results even when comparatively complicated tasks from microstrip circuits are to be solved. The analytical expressions obtained are relatively simple and they enable an objective interpretation of results. For the dielectrics current used in contemporary microwave integrated techniques ($\epsilon_r <$ 30) the accuracy of our calculation is quite satisfactory and comparable with the accuracy of other, more complicated and more time consuming calculating methods.

The method described above can be generalized to cover solutions of multilayer microstrip structure with more than three dielectric layers. While in these cases the complexity of numerical

calculations according to [2] and [4] grows very rapidly and the time necessary for the calculation of the line parameters becomes considerably longer, our calculation does not become more complicated, because it uses the same relations as given above.

References

[1] K. C. Gupta, R. Garg, and I. J. Bahl, *Microstrip Lines and Slot-Lines*. Dedham, MA: Artech House, 1979.

[2] E. Yamashita, "Variational method for the analysis of microstrip-like transmission lines," *IEEE Trans. Microwave Theory Tech.*, vol. MTT-16, no. 8, pp. 529–535, 1968.

[3] E. Yamashita and K. Atsuki, "Strip line with rectangular outer conductor and three dielectric layers," *IEEE Trans. Microwave Theory Tech.*, vol. MTT-18, no. 5, pp. 238–244, 1970.

[4] A. Farrar and A. T. Adams, "Multilayer microstrip transmission lines," *IEEE Trans. Microwave Theory Tech.*, vol. MTT-22, no. 10, pp. 889–891, 1974.

[5] H. A. Wheeler, "Transmission line properties of parallel wide strips by a conformal mapping approximation," *IEEE Trans. Microwave Theory Tech.*, vol. MTT-12, no. 3, p. 280, 1964.

[6] ——, "Transmission line properties of parallel strips separated by a dielectric sheet," *IEEE Trans. Microwave Theory Tech.*, vol. MTT-13, no. 2, p. 172, 1965.

[7] W. J. Getsinger, "Microstrip dispersion model," *IEEE Trans. Microwave Theory Tech.*, vol. MTT-21, no. 1, p. 34, 1973.

[8] B. E. Spielman, "Dissipation loss effects in isolated and coupled transmission lines," *IEEE Trans. Microwave Theory Tech.*, vol. MTT-25, no. 8, p. 648, 1977.

[9] P. Pramanick and P. Bhartia, "Computer-aided design models for millimeter-wave finlines and suspended-substrate microstrip lines," *IEEE Trans. Microwave Theory Tech.*, vol. MTT-33, no. 12, p. 1429, 1985.

Analysis of a New Configuration of Coplanar Stripline

J. S. McLean and Tatsuo Itoh

Abstract—**A new configuration of coplanar stripline is presented and analyzed. This configuration is derived by augmenting coplanar stripline with electrically wide lateral ground planes on either side of the balanced pair of signal lines. The ground planes should reduce line-to-line coupling in complex circuits and eliminate the TE_0 parasitic dielectric slab waveguide mode. Also, the spacing from signal lines to ground planes may be adjusted to change the characteristic impedance. Spectral domain analysis is used to calculate the dispersion characteristics of this transmission line. Furthermore, analytical expressions for quasi-static values of the propagation constant and characteristic impedance of the line are presented. This configuration of CPS should be useful for balanced high impedance lines in MMIC and high speed digital circuits.**

Introduction

Coplanar stripline (CPS), like coplanar waveguide (CPW), offers flexibility in the design of complex planar microwave/millimeterwave circuitry in that series and shunt connections can be made easily. In addition, CPS is useful in fabricating lines with high characteristic impedances as it is easier to realize a high impedance with CPS than CPW [1]. Furthermore, it is a balanced transmission line which is useful for balanced circuits such as mixers and with differential drivers such as those used in some high-speed digital applications. The main drawback to CPS is that, due to the lack of the shielding which is inherent in CPW, stray coupling to other lines can occur. Furthermore, in conventional CPS, the lack of a ground plane allows the existence of two parasitic dielectric slab waveguide modes, the TM_0 and the TE_0, which have no cutoff frequency [2]. The TE_0 mode couples strongly to the fundamental CPS mode at discontinuities (but not on uniform CPS line) causing losses and extraneous coupling [3]. This is because the electric fields of the TE_0 slab mode and the fundamental mode of CPS are both parallel to the dielectric interface. In this short paper, we examine the dispersion characteristics of a new configuration of coplanar stripline which eliminates some of the disadvantages of conventional CPS. In this configuration, the stripline is bounded on either side with semi-infinite ground planes as shown in Fig. 1. Thus, this CPS configuration is similar to CPW with laterally infinite ground planes. In practice, of course, the ground planes are of finite width. However, the analysis should be a very good approximation to the case in which the ground planes are electrically wide. One advantage provided by the ground planes is that line-to-line coupling, which is considered to be a drawback to conventional CPS, is reduced. Also, the TE_0 dielectric slab waveguide mode is eliminated by the ground planes, thus reducing losses at discontinuities. A TM_0 surface wave mode which has no cutoff frequency can still exist, but this is not a serious problem since the TM_0 fields are predominantly prependicular to those of the CPS mode. Finally, the spacing between the signal lines and the ground planes may be adjusted in order to modify the characteristic impedance of the line. The dispersion characteristics of this new CPS configuration have been calculated using the spectral domain technique. These dispersion characteristics are compared with those of conventional CPS which were also calculated using spectral domain analysis. Finally, analytical expressions for approximate quasi-static values of the propagation constant and characteristic impedance of this configuration of CPS are given. These expressions were derived from the conformal mapping analysis used by Ghione [4] to analyze finite ground plane coplanar waveguide.

Numerical Method

The spectral domain analysis of the modified configuration of coplanar stripline shown in Fig. 1 is similar to that used by Itoh [5] to analyze coplanar waveguide with semi-infinite ground planes. The CPW analyzed in [5] can be visualized as two coupled slots in an odd mode whereas the modified CPS we consider here can be visualized as three coupled slots in an even mode. To briefly summarize, the electric field integral equation is transformed into the Fourier transform domain to yield two coupled algebraic equations relating the Fourier transforms of the components of the tangential electric field to those of the electric current density at the dielectric interface. That is:

$$\tilde{Y}_{xx}(\alpha, \beta)\tilde{E}_x(\alpha, \beta) + \tilde{Y}_{xz}(\alpha, \beta)\tilde{E}_z(\alpha, \beta) = \tilde{J}_x(\alpha, \beta) \quad (1)$$

$$\tilde{Y}_{zx}(\alpha, \beta)\tilde{E}_x(\alpha, \beta) + \tilde{Y}_{zz}(\alpha, \beta)\tilde{E}_z(\alpha, \beta) = \tilde{J}_z(\alpha, \beta) \quad (2)$$

where $\tilde{Y}_{xx}(\alpha, \beta) \cdots \tilde{Y}_{zz}(\alpha, \beta)$ are components of the spectral domain Green's function, $\tilde{E}_z(\alpha, \beta)$ and $\tilde{E}_x(\alpha, \beta)$ are the Fourier trans-

Manuscript received July 22, 1991; revised October 28, 1991. This work was supported by the U.S. Army Research office under contract DAAL-03-88-K-0005.

J. S. McLean is with the Department of Electrical and Computer Engineering, University of Wisconsin at Madison, 1415 Johnson Drive, Madison, WI 53706-1691.

T. Itoh is with the Department of Electrical Engineering, The University of California at Los Angeles, 66-147A Engineering IV, Los Angeles, CA 90024-1594.

IEEE Log Number 9106039.